J Mater Sci (2007) 42:5437–5441
DOI 10.1007/s10853-006-0785-1

Effects of milling conditions on hydrogen storage properties of graphite

Zhenguo Huang · Andrzej Calka · Huakun Liu

Received: 23 May 2006 / Accepted: 11 August 2006 / Published online: 23 March 2007

Abstract Two milling modes (shearing and impact) were applied to investigate the hydrogen storage properties of graphite. It was found that the shearing mode leads to 0.613 wt.% hydrogen absorbed in graphite, while impact mode leads to 2.718 wt.%. X-ray diffraction was used to investigate the structure of the as-milled and subsequent annealed samples. Differential scanning calorimetry was used to study thermally induced transformations in the as-milled samples. Infrared spectrometry was carried out to investigate the interaction between carbon and hydrogen atoms. Results are compared and discussed in conjunction with Laser desorption time-of-flight mass spectrometry results obtained earlier.

Introduction

As a very promising hydrogen storage candidate, graphite has attracted considerable research interest. However, all the results related to hydrogen absorption properties are very scattered, ranging from around 0 to 67 wt.% [1–5]. Since most of the results were obtained through ball milling, the discrepancies are presumably due to the large variation of ball milling conditions. The absorption properties of milling products are dependent on many factors such as milling atmosphere, the duration of milling, the materials of the milling media, and the energies applied, etc. All the above experimental parameters are quite different from each other as recorded in the publications.

Generally, hydrogen atoms are trapped at two sites: (1) graphite inter-layers through solitary carbon dangling bonds and 2) the edge surface of a crystallite through carbon dangling bonds [5–7]. Mechanical milling contributes to the formation of dangling carbon bonds [8–10], therefore, hydrogen storage capacities of graphite should be enhanced by ball milling. Additionally, hydrogen solubility, diffusivity and desorption properties in graphite are defect related [11–15], and these defects can also be generated through mechanical milling [16–19]. So far, hydrogen storage properties of graphite resulting from ball milling have been mainly investigated by using two types of high energy mills: planetary (Fritsch) and vibrational (Spex), in which the movement of the grinding balls is very chaotic, which leads to the generation of a large spectrum of local milling energies and in consequence to a spectrum of local absorption rates. In order to control the milling energy, the movement of the grinding balls has to be controlled [20, 21]. In experimental practice it is convenient to have the ability to adjust from low-energy shearing to high-energy impact to allow control of the milling energy and to address potential mill processing problems, such as metal cold welding and contamination from milling media.

More investigations on graphite are needed for better understanding of the mechanisms of hydrogen adsorption and desorption, to obtain a reliable capacity and ultimately safe technical implementations. In the present work, two milling modes (shearing and impact) were applied with the aim of clarifying the influence of the milling mode on the hydrogen storage capacity of graphite.

Z. Huang (✉) · H. Liu
Institute for Superconducting and Electronic Materials, University of Wollongong, Wollongong, NSW 2522, Australia
e-mail: zh104@uow.edu.au

A. Calka
Faculty of Engineering, University of Wollongong, Wollongong, NSW 2522, Australia

Experimental

Graphite powder with a purity of 99.95% was milled under hydrogen in a magneto-mill, Uni-Ball-Mill 5 [20] under elemental milling modes such as impact and shearing (Fig. 1). The milling cylinder was evacuated and purged several times using helium firstly, and then filled with hydrogen gas up to 500 kPa pressure. The milling time was 100 h. For comparison, graphite powder was milled in helium atmosphere using the same milling conditions.

In the shearing mode (Fig. 1a), the balls both rotate and oscillate around an equilibrium position at the bottom of the milling cylinder in a strong magnetic field. In the impact mode, the ball movement during the milling process is confined to the vertical plane by the cylinder walls and is controlled by an external magnetic field (Fig. 1b). In both cases, the magnetic field is generated by FeNdB magnets. The intensity and direction of the magnetic field can be externally adjusted, allowing the ball trajectories and impact energy to be varied in a controlled manner [20]. The sample ball milled in hydrogen using the shearing mode was designated as SH and the one using the impact mode as IH. In the same way, the sample ball milled in helium by the shearing mode was designated as SHe and by the impact mode as IHe.

X-ray diffraction (XRD) patterns of the as-milled and annealed powders were obtained through a Philips PW 1730 generator and diffractometer using Cu Kα radiation (λ = 0.15418 nm) and a graphite monochromator. Differential scanning calorimetry (Perkin-Elmer DSC-4) was performed on the samples, with an argon flow rate of 70 mL/min at a heating rate of 20 °C/min up to 500 °C. To determine the hydrogen content absorbed during ball milling, combustion elemental analysis was performed on a CHN Carlo Erba Elemental Analysis Model 1106. The infrared absorbance was recorded using a Nicolet Avatar 360 FTIR spectrometer with an OMNI-sampler installed.

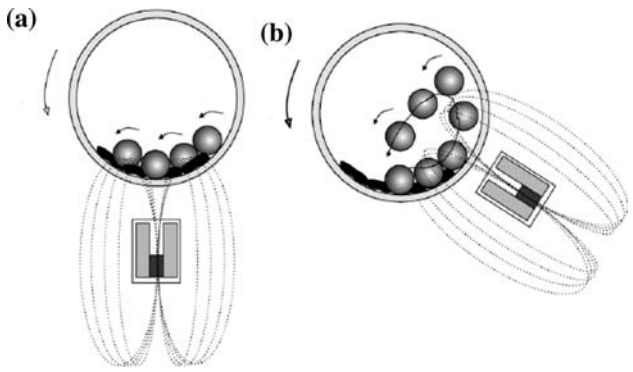

Fig. 1 The Uni-Ball-Mill 5 with the FeNdB external magnets operating in the shearing (**a**) and the impact (**b**) modes of milling [20]

Results and discussion

The XRD pattern in Fig. 2b shows that the graphitic structure still exists in the as-milled product after milling by shearing mode, and the grain size estimated according to Scherrer equation is about 10 nm, which indicates that shearing mode is effective in the formation of a nanostructured layered structure. The broadening of the (002) reflection peak is probably due to the following reasons: (1) the nanoscale grain size and (2) microstresses induced during milling. The (002) reflection peak disappears following the annealing process (Fig. 2c–f), which means that the graphitic structure is metastable and the layered structure exfoliates upon heating. The samples annealed at lower temperatures (240 °C, 300 °C) are predominantly nanostructured. The existence of austenite and magnetite (Fig. 2f) indicates contamination from the milling media.

The graphitic structure disappeared after milling graphite using impact mode (Fig. 3a), presumably due to the high degree of deformation caused by strong collisions between balls during milling. The high energy milling mode (impact) led to some degree of iron contamination in the formation of iron carbide, however, contamination in the as-milled SH (Fig. 2b) is not detected. The presence of iron, austenite also indicated that the high-energy milling process involves more contamination, which is confirmed through Mossbauer spectroscopy measurements [22]. The annealed IHs also became nanostructured (Fig. 3b–d), which reveals similar structural evolution to that of the annealed SHs.

The DSC traces illustrate the distinctive thermal properties of the IH and SH. There are a series of small exothermic-like peaks for IH, while only two relatively large peaks and another small peak are found for SH. Two small peaks were enlarged for further study (insets in Fig. 4). They are each revealed as one small endothermic peak closely followed by one large exothermic peak. The possible origins of the peaks will be discussed later in the paper.

The combustion elemental analysis showed that the hydrogen content reached 0.613 and 2.718 wt.% for the SH and IH samples, respectively. From the application point of view, the high-energy impact mode is more favourable. It is well known that carbon dangling bonds are defect related [8–10]. High-energy impact in this experiment led to more defects than low-energy shearing, and consequently impact mode improves the hydrogen storage capacity. After the above DSC experiment, there was about 0.30 wt.% and 2.34 wt.% of hydrogen left in the SH and IH samples, respectively.

Figure 5 shows DSC traces obtained from the as-milled graphite in helium. The purpose of this experiment was to investigate thermal effects due to the structural evolution of

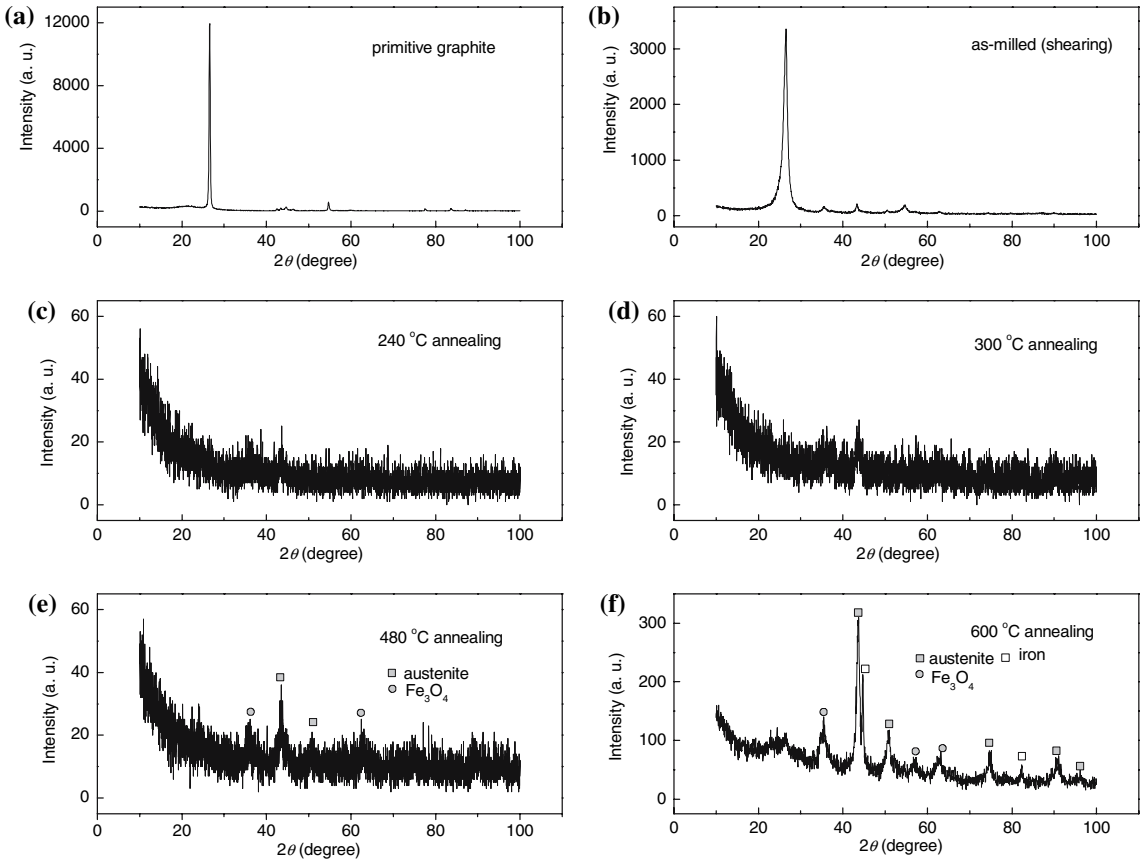

Fig. 2 XRD patterns obtained from pristine graphite, as-milled graphite (shearing mode) in hydrogen, and the annealed products at different temperatures

Fig. 3 XRD patterns obtained from as-milled graphite (impact mode) in hydrogen and subsequent annealed products at different temperatures

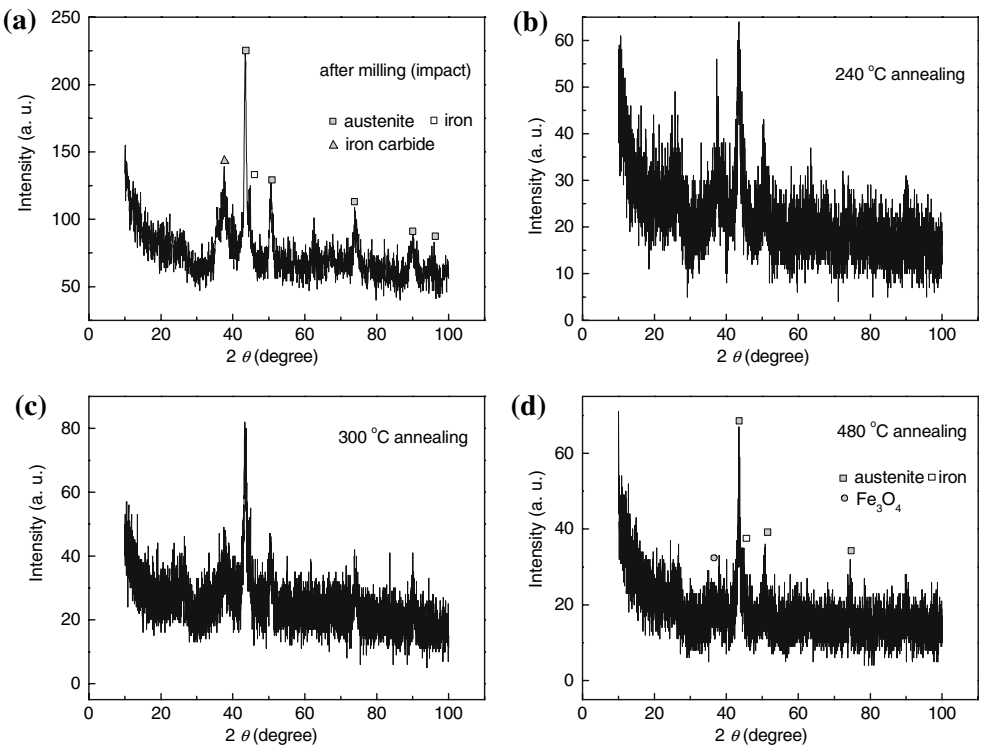

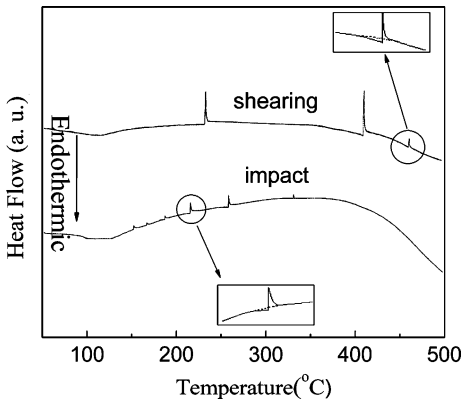

Fig. 4 DSC traces of the graphite milled in hydrogen through the shearing and impact mode

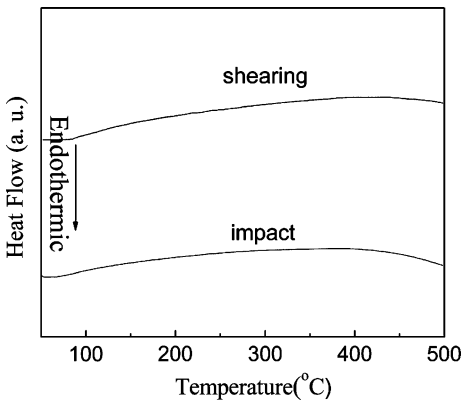

Fig. 5 DSC traces of graphite milled in helium through the shearing and impact mode

ball milled graphite and distinguish these effects from effects due to carbon–hydrogen interaction. There is no clear heat absorption or desorption for either sample. Since nanostructural graphite recrystallizes at above 800 °C [23], the effect of different milling modes on the structural evolution presumably can not be displayed at the temperature range applied in this experiment. Taking into account the different milling atmospheres, the series of endothermic and exothermic-like peaks obtained from SH and IH (Fig. 4) are due to the interaction between carbon and hydrogen, since all the other milling conditions remained the same.

The possible composition of the as-milled samples is investigated through Laser desorption time-of-flight mass spectrometry [22]. The results revealed a variety of bare carbon clusters as well as hydrogenated carbon clusters. The likely hydrogenated carbon clusters are shown in Table 1. The formation of hydrogenated carbon clusters is associable with the milling mode, with impact leading to many kinds, and shearing resulting in only two.

Table 1 The possible hydrogenated carbon clusters observed in the mass spectra of the graphite milled under hydrogen atmosphere in the *impact* and the *shearing* modes [22]

C_nH_x impact mode	C_nH_x shearing mode
C_5H_4	C_5H_4
C_7H_1	
C_7H_2	C_7H_2
C_7H_3	
C_8H_1	
C_8H_3	

In the light of the compositions listed in Table 1, the exothermic-like peaks can be interpreted. As can be seen in the insets of Fig. 4, the small peak actually is an endothermic peak followed by an exothermic peak, which is presumably due to the hydrogen desorption from the hydrogenated carbon cluster and the succeeding carbon atom re-arrangement with the formation of a bigger carbon cluster [24, 25]. There are six types of hydrogenated carbon clusters in the IH, and the desorption temperatures are different, as can be seen from the different positions of the small peaks. On the contrary, only two types of hydrogenated carbon clusters exist in the SH, and as a result, only two large peaks and another small peak are visible.

Graphite itself has been intensively studied as a very promising hydrogen storage medium. Based on this, we would expect to observe some C–H bonding in the as-milled samples. To confirm this hypothesis, infrared absorbance of the composites was recorded (Fig. 6), because this technique gives information on bonding configuration and on hydrogenated bonds [26]. The strong signal below 700 cm^{-1} originates from the equipment itself. The main features of the spectra are associated with CO_2 and H_2O [27], and the characteristic stretching mode of the C–H bond at 2800–3000 cm^{-1} is not visible in the

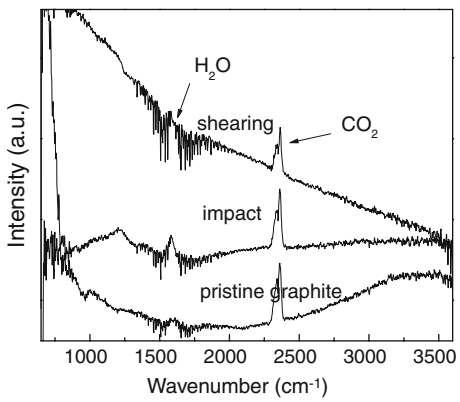

Fig. 6 Infrared spectra of graphite obtained by milling in hydrogen through the shearing mode and impact mode. The spectrum of pristine graphite is also shown

spectra [28]. It has to be noted that graphite can also store hydrogen via the formation of hydrogenated carbon cluster when it was milled in hydrogen. The correlation between carbon and hydrogen in the samples is presumably not classical C–H bonding. The molecular formulas derived from the mass spectrometry also give a clue, since they are very dissimilar to classical hydrocarbons.

Conclusion

On the basis of the above results one can conclude that different ball milling modes lead to dissimilar amounts of hydrogen trapped by carbon clusters. Additionally, the formation of hydrogenated carbon clusters also depends on the milling mode applied, with the sample obtained through the high-energy mode consisting of a variety of carbon clusters, in contrast to only two existing in the sample obtained through the low-energy mode.

The exothermic-like peak actually is a combination of one small endothermic peak and one large exothermic one, which is assumed to be due to hydrogen desorption and subsequent re-arrangement of carbon atoms. The carbon hydrogen interaction seems not to be classical C–H bonding on the basis of the IR results.

Acknowledgement Financial support from the Australian Research Council through an ARC Discovery project (DP 0449660) is gratefully acknowledged.

References

1. Dillon AC, Jones KM, Bekkedahl TA, Kiang CH, Bethune DS, Heben MJ (1997) Nature 386:377
2. Kajiura H, Tsutsui S, Kadono K, Kakuta M, Ata M, Murakami Y (2003) Appl Phys Lett 82:1105
3. Chambers A, Park C, Terry R, Baker K, Rodriguez NM (1998) J Phys Chem B 102:4253
4. Züttel A, Sudan P, Mauron Ph, Kiyobayashi T, Emmenegger Ch, Schlapbach L (2002) Int J Hydrogen Energy 27:203
5. Ichikawa T, Chen DM, Isobe S, Gomibuchi E, Fujii H (2004) Mater Sci Eng B 108:138
6. Atsumi H, Tauchi K (2003) J Alloys Comp 356–357:705
7. Orimo S, Majer G, Fukunaga T, Zuttel A, Schlapbach L, Fujii H (1999) Appl Phys Lett 75:3093
8. Fukunaga T, Nagano K, Mizutani U, Wakayama H, Fukushima Y (1998) J Non-Cryst Solids 232–234:416
9. Chen Y, Gerald JF, Chadderton LT, Chaffron L (1999) Appl Phys Lett 4:2782
10. Kaneshenko SL, Gorodetsky AE, Chernikov VN, Markin AV, Zakharov AP, Doyle BL, Wampler WR (1996) J Nucl Mater 233–237:1207
11. Haasz AA, Franzen P, Davis JW, Chiu S, Pitcher CS (1995) J Appl Phys 77:66
12. Davis JW, Haasz AA (1995) J Nucl Mater 220–222:832
13. Atsumi H, Iseki M, Shikama T (1996) J Nucl Mater 233–237:1128
14. Gotoh Y (1997) J Nucl Mater 248:46
15. Huang JY (1999) Acta Mater 7:1801
16. Huang JY, Yasuda H, Mori H (1999) Chem Phys Lett 303:130
17. Chen Y, Gerald JF, Chadderton LT, Chaffron L (1999) Appl Phys Lett 74:2782
18. Ong TS, Yang H (2000) Carbon 38:2077
19. Chen XH, Yang HS, Wu GT, Wang M, Deng FM, Zhang XB, Peng JC, Li WZ (2000) J Cryst Growth 218:57
20. Calka A, Radlinski AP (1991) Mater Sci Eng A 134:1350
21. Calka A, Nikolov JI (1995) NanoStructured Mater 6:409
22. Smolira A, Szymanska M, Jartych E, Calka A, Michalak L (2005) J Alloys Comp 402:256
23. Orimo S, Matsushima T, Fujii H, Fukunaga T, Majer G (2001) J Appl Phys 90:3
24. Huang ZG, Calka A and Liu HK, J Mater Sci, doi: 10.1007/s10853-006-0382-3
25. Calka A, Nikolov JI, Williams JS (1996) Mater Sci Forum 225–227:527
26. Musumeci P, Calcagno L, Makhtari A, Baeri P, Compagnini G, Pirri CF (2000) Nucl Instr Meth Phys Res B 166–167:404
27. Welham NJ, Berbenni V, Chapman PG (2003) J Alloys Comp 349:255
28. Popescu B, Tagliaferro A, Da Zan F, Davis EA (2000) J Non-Cryst Solids 266–269:803